

S9. Transport Analysis of ECH Overlapped NBI Plasmas

Funaba, H., Shimozuma, T., Kubo, S., Narihara, K., Ida, K., Takeiri, Y., Nagayama, Y., Inagaki, S., Murakami, S., Yokoyama, M., Ohya, N., LHD Experimental Group

The electron temperature, T_e , profile with a high central $T_e(0)$ and a steep gradient, ∇T_e , was observed on LHD in both ECH plasmas and low density NBI plasmas with overlapping of the strongly focused ECH. Local transport analysis is carried out in order to clarify whether any transport improvement appeared or not in LHD associated with this high central T_e .

Figure 1 shows four profiles of T_e in the ECH overlapped NBI plasmas with different n_e and a NBI-only plasma. These plasmas were produced under the conditions of $R_{ax} = 3.75$ m and $B = 1.52$ T. The steep ∇T_e appears in the low density cases (\bullet , Δ) at the $\rho < 0.2$ region. The experimental thermal diffusivities of electrons, χ_e , are evaluated by the local transport analysis using an one-dimensional transport code, PROCTR. χ_e^{exp} in the NBI-only case is about $12 \text{ m}^2/\text{s}$ at the center and it gradually decreases towards the edge as seen in Fig.2. The magnitude of χ_e^{exp} in the high density NBI with ECH plasma becomes large at the central region because of the increase in the deposition power to electrons. On the other hand, the central χ_e^{exp} was reduced in the case of the low density NBI with ECH plasma. The neoclassical χ_e^{neo} with the radial electric field, E_r^{neo} , are calculated and they are smaller than χ_e^{exp} by about one order. Figure 3 shows the power balance of electrons and ions in a NBI with ECH plasma (Δ in Fig.1). The deposition power profiles of NBI, $p_{NBI}^e(\rho)$ and $p_{NBI}^i(\rho)$, are given by the calculation results from a three-dimensional Monte Carlo simulation code. The absorbed power of ECH, $p_{ECH}(\rho)$, is calculated by the ray-tracing method. p_{ECH} is localized at the resonance position of the normalized minor radius $\rho \simeq 0.1$ and its peak value exceeds 1 MW/m^3 . On the other hand, p_{NBI}^e has a broad profile and it is usually less than 100 kW/m^3 .

The transport coefficients which are derived by the steady state analysis are still ambiguous at the central region of $\rho < 0.1$ as p_{ECH} shows small value at the vicinity of $\rho = 0$. In order to evaluate χ_e near the center, the temporal development of T_e after ECH switching off is calculated with assuming a certain χ_e and it is compared with the ECE signals (T_e^{ECE}) as shown in Fig.4. The magnitude of T_e^{ECE} is calibrated by the Thomson scattering data here. In the higher P_{ECH} case, the T_e profile has a steep gradient and the decay times, τ_d , of T_e^{ECE} are more than 100 ms at the central region, while no steep gradient was observed and $\tau_d \simeq 20$ ms in the lower P_{ECH} case. The dotted curve

in Fig.4 shows a example of the results of the calculation by using χ_e^{exp} . The decay time of this case is smaller than that of T_e^{ECE} . The dashed curves in Fig.4 are the calculation results by using some assumed χ_e which are selected in order to reproduce the time development of T_e^{ECE} . Although these simulation results are not completely agree with the experimental data, the longer decay times of $50 \sim 100$ ms can be reproduced. The assumed χ_e is less than $0.01 \text{ m}^2/\text{s}$ at $\rho \simeq 0$ and $0.13 \text{ m}^2/\text{s}$ at $\rho \simeq 0.1$. It may be considered that these small χ_e values also indicate some improvement of electron thermal transport at the center.

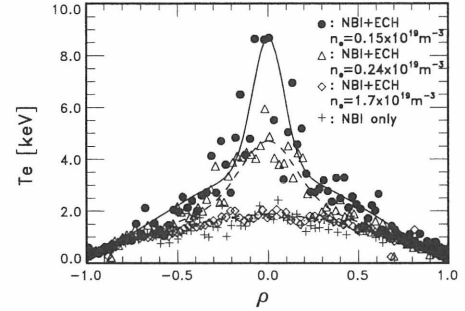


Fig. 1. T_e profiles of NBI with ECH plasmas.

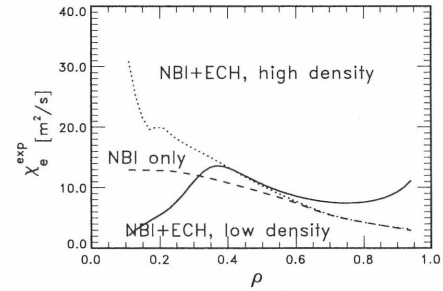


Fig. 2. χ_e of NBI with ECH plasmas.

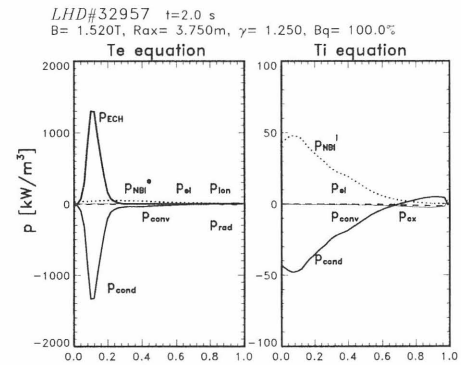


Fig. 3. The power balance of electrons and ions.

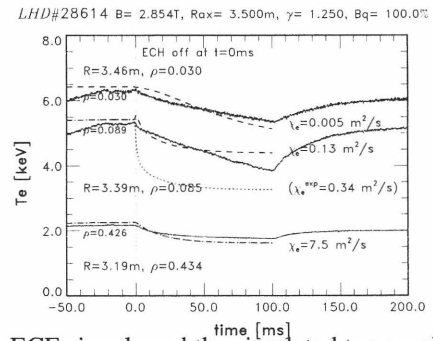


Fig. 4. ECE signals and the simulated temporal development of T_e .